



Contents lists available at ScienceDirect

Asian Pacific Journal of Tropical Medicine

journal homepage: www.elsevier.com/locate/apjtm



Document heading doi: 10.1016/S1995-7645(14)60052-3

## Inhibitory effect of humanized anti-VEGFR-2 ScFv-As<sub>2</sub>O<sub>3</sub>-stealth nanoparticles conjugate on growth of human hepatocellular carcinoma: *in vitro* and *in vivo* studies

Xiang-Bao Yin\*, Lin-Quan Wu, Hua-Qun Fu, Ming-Wen Huang, Kai Wang, Fan Zhou, Xin Yu, Kai-Yang Wang

Department of Hepatobiliary Surgery, 2nd Affiliated Hospital of Nanchang University, Nanchang, Jiangxi Province, China

### ARTICLE INFO

#### Article history:

Received 10 December 2013

Received in revised form 15 January 2014

Accepted 15 February 2014

Available online 20 May 2014

#### Keywords:

Anti-VEGFR-2 single-chain antibody conjugate  
As<sub>2</sub>O<sub>3</sub> stealth nanoparticles  
Hepatocellular carcinoma

### ABSTRACT

**Objective:** To investigate the inhibitory effect of humanized anti-VEGFR-2 ScFv-As<sub>2</sub>O<sub>3</sub>-stealth nanoparticles conjugate on growth of human hepatocellular carcinoma both *in vitro* and *in vivo*, which may be a potential agents with sensitivity and targeting ability for human hepatocellular cancer. **Methods:** Humanized anti-VEGFR-2 ScFv-As<sub>2</sub>O<sub>3</sub>-stealth nanoparticles conjugate was previously constructed using ribosome display technology and antibody conjugate technology. In this combined *in vitro* and *in vivo* study, the inhibitory effects of anti-VEGFR-2 ScFv-As<sub>2</sub>O<sub>3</sub>-stealth nanoparticles conjugate on tumor growth, invasion, and metastasis was observed with human liver carcinoma cell line Bel7402 and normal cell L02 by MTT assay, Tanswell assay, Hoechst33258 staining, and DNA ladder analysis. The anticancer activity and distribution of anti-VEGFR-2 ScFv-As<sub>2</sub>O<sub>3</sub>-stealth nanoparticles was then verified in a mouse model of Bel7402 xenografts. **Results:** Anti-VEGFR-2 ScFv-As<sub>2</sub>O<sub>3</sub>-stealth nanoparticles significantly inhibited the proliferation of Bel7402 in the 3-(4,5-dimethylthiazol-2-yl)-2,5-diphenyltetrazolium bromide assay while had almost no effects on L02 cells. And the apoptosis inducing effects were proved by Hoechst33258 staining and DNA ladder analysis. Transwell assay found that the drug also inhibited the metastasis ability of tumor cells. Furthermore, anti-VEGFR-2 ScFv-As<sub>2</sub>O<sub>3</sub>-stealth nanoparticles significantly delayed the growth of Bel7402 xenografts after administration (92.9%), followed by As<sub>2</sub>O<sub>3</sub>-stealth nanoparticles, anti-VEGFR-2 ScFv, and As<sub>2</sub>O<sub>3</sub> (61.4%, 58.8%, 20.5%,  $P < 0.05$ ). The concentration of As<sub>2</sub>O<sub>3</sub> in anti-VEGFR-2 ScFv-As<sub>2</sub>O<sub>3</sub>-stealth nanoparticles group was more selectively. **Conclusions:** Anti-VEGFR-2 ScFv-As<sub>2</sub>O<sub>3</sub>-stealth nanoparticles is a potent and selective anti-hepatocellular carcinoma agent which could inhibit the growth of liver cancer as a targeting agent both *in vitro* and *in vivo* and also significantly inhibit angiogenesis.

## 1. Introduction

Hepatocellular carcinoma (HCC) is one of the most common malignancies, with an increasing incidence all over the world. Traditional clinical treatments for hepatocellular carcinoma include surgery, chemotherapy and radiotherapy. And with advances in surgical techniques

and instrumentation and the development of molecular-target drugs, a number of potentially curative treatments have become available than ever before<sup>[1–3]</sup>. The therapeutic effect of liver resection was satisfied only in a small portion of patients with poor prognosis. Most HCC patients may have cirrhosis as well as hypersplenism and peripheral blood cells reduction in the meantime, so they may be unbearable for systemic chemotherapy while radiation therapy also works only for patients with good liver function without complications such as cirrhosis, ascites, jaundice, or any distant metastasis, which limits the application of the therapy methods<sup>[4–6]</sup>.

Recent years, with the development in molecular mechanisms about tumor cell growth, proliferation and

\*Corresponding author: Dr Xiang-Bao Yin, Department of hepatobiliary surgery, 2nd affiliated hospital of Nanchang University, No.1 Minde Road, Nanchang, Jiangxi Province, 330006, China.

E-mail: yxb115@sina.com

Foundation project: This project was supported by Natural Science Foundation of China (81060187) and the Natural Science Foundation of Jiangxi Province (2008GQY0050).

apoptosis, the molecular characteristics of tumors are better understood and it makes it possible for targeted cancer therapy that blocks the growth of cancer cells by interfering with specific targeted molecules or cytokines needed for carcinogenesis and tumor growth<sup>[7]</sup>. Increased understanding of the molecular mechanisms involved in cancer development has led to the identification of numerous novel targets for drug developments. Targeted therapy focus on certain specific signal transduction molecules including crucial molecules involved in cell proliferation and apoptosis, cell invasion, metastasis, cell-cycle control, and tumor-related angiogenesis, and in recent years, antibody-drug conjugates have brought us into a new era for personalized cancer treatment which can improve the effects of anti-cancer drugs such as cytotoxic drugs while reducing their toxicity to normal organs<sup>[8,9]</sup>.

Tumor cells could produce angiogenic factor vascular endothelial growth factor (VEGF), which can bind vascular endothelial cell surface receptors, resulting in a variety of biological effects, thereby promoting tumor progression<sup>[10]</sup>. Arsenic trioxide ( $As_2O_3$ ) has been used medicinally in traditional Chinese medicine for thousands of years, and it has been used for treatment of cancer for several hundred years of history, and its therapeutic use in leukaemia has been described a century before<sup>[11]</sup>. Until now, it has been reported to be used for the treatment of esophageal cancer, breast cancer, gastric carcinoma, colon cancer, cervical cancer, prostate cancer and other solid tumors<sup>[12-14]</sup>. But as a highly toxic drug, the application of arsenic trioxide is limited in clinical due to its poor targeting ability to tumor cells, which lead to great toxicity to normal cells of the body<sup>[11,15]</sup>. Our group previously have built anti-VEGFR-2 ScFv modified  $As_2O_3$ -stealth nanoparticles (anti-VEGFR-2 ScFv- $As_2O_3$ -stealth nanoparticles) using molecular coupling technology to, in order to delivery  $As_2O_3$  to targeted tumor cells. In this study, we investigated the inhibitory effect of humanized anti-VEGFR-2 ScFv- $As_2O_3$ -stealth nanoparticles conjugate on growth of human hepatocellular carcinoma both *in vitro* and *in vivo*.

## 2. Materials and methods

### 2.1. Cell culture and MTT assay

The human hepatoma cancer cell line Bel7402 was purchased from the American Type Cell Culture (USA). Bel7402 cells were maintained in RPMI-1640 supplemented with 10% (v/v) heat-inactivated fetal bovine serum, penicillin-streptomycin (100 IU/mL-100 g/mL), 2 mM glutamine, and 10 mM Hepes buffer at 37 °C in a humid atmosphere (5%-95%  $CO_2$ ). The inhibitory effect of different drugs on Bel7402 cell proliferation was estimated by the 3-(4,5-dimethylthiazol-2-yl)-2,5-diphenyl-tetrazolium bromide (MTT, Sigma-Aldrich, USA) assay<sup>[16]</sup>.

### 2.2. Transwell assay

Cell migration and invasion were assayed using a transwell chamber (Millipore, USA) with and without Matrigel (BD, Franklin Lakes, USA). For the invasion assay, a transwell chamber was placed into a 24-well plate and was coated with 30  $\mu$  L Matrigel and was incubated for forty minutes at 37 °C. Cells were trypsinized and seeded in chambers at the density of  $1 \times 10^6$  cells per ml and cultured in medium with RPMI 1640 medium with 2% serum, while 500  $\mu$  L of 10% FBS-1640 was added to the lower chamber. Twenty-four hours later, migrated cells were fixed with 100% methanol for 30 min. Non-migrated cells were removed by cotton swabs. Then cells on bottom surface of the membrane were stained by crystal violet for 20 min. Cell images were obtained under a phase-contrast microscope (Olympus, Tokyo, Japan)<sup>[17]</sup>.

### 2.3. Hoechst33258 staining morphological studies

Variations in cell morphology were analyzed by fluorescence microscopy. Cells attached to coverslips were fixed in cold methanol for 5 min, air dried, stained with Hoechst-33258 (1  $\mu$  L Hoechst 33258 in 100  $\mu$  L PBS) and observed under Olympus BX61 microscope.

### 2.4. DNA ladder analysis of DNA fragmentation

Fragmentation of DNA was analyzed by agarose gel electrophoresis during apoptosis. Bel 7402 cells were treated with different drugs for 4 h, then irradiated for 10 min with uorescent light, and incubated for 4 h or overnight. DNA was extracted with phenol/chloroform and precipitated in ethanol. The extracted DNA was separated by agarose gel electrophoresis (1.5% agarose gel containing 0.4  $\mu$  g/mL ethidium bromide, 100 V, 1 h) and visualized under UV light<sup>[18]</sup>.

### 2.5. *In vivo* activity of humanized anti-VEGFR-2 ScFv- $As_2O_3$ -nanoparticles

Six-week-old male nude (nu/nu) BALB/c mice (SLRC Laboratory Animal, Shanghai, China) weighing 18-20 g were used for all experiments. Tumor models were established by a subcutaneous injection of  $1 \times 10^7$  Bel7402 cells into the back of mice. Tumor volumes were estimated according to the formula:  $0.5 \times ab^2$  (a, length; b, width). When tumors reached about 100  $mm^3$ , the mice were randomly assigned to five groups (8 mice per group): intravenous injection of anti-VEGFR-2 ScFv- $As_2O_3$ -stealth nanoparticles (group A, containing 5 mg/kg of equivalent  $As_2O_3$ ),  $As_2O_3$  nanoparticles (group B, containing 5 mg/kg of equivalent  $As_2O_3$ ), anti-VEGFR-2 ScFv (group C, containing an identical antibody concentration as anti-VEGFR-2 ScFv- $As_2O_3$ -nanoparticles injected),  $As_2O_3$  solution (group D, 5 mg/kg) and saline (group E, received 0.2 mL *ip.* injections of saline). The drugs were administered once a day for 5 consecutive days.

Tumor volumes were measured every 2 d after termination

of drug administration. 12 days after drug administration, peripheral blood of the mice were collected to detect leukocytes [white blood count (WBC)] and platelets PLT levels, then the mice were sacrificed, and tumors were excised and weighed.

## 2.6. Immunohistochemistry and microvascular density (MVD)

After sacrifice, the tumor tissues were removed from each mouse. Some of the tumor tissues were subsequently fixed in formalin, embedded in paraffin and stained with hematoxylin and eosin (H&E) for further investigation.

Angiogenesis in tumor tissues was evaluated according to MVD counting by staining with CD34. After deparaffinization and antigen retrieval, endogenous peroxidase was blocked. The sections were washed and non-specific binding was blocked and then sections were incubated with CD34 primary antibody and then treated with biotinylated anti-immunoglobulin.

## 2.7. TUNEL

Apoptotic cells in tumor tissues were determined by terminal deoxynucleotidyl transferase-mediated dUTP nick end labeling (TUNEL) staining using an in situ cell death detection kit (Roche, Mannheim, Germany) using serial 4  $\mu$ m sections cut from paraffin-embedded tumor tissues. The staining was performed according to the manufacturer's instructions. The proportion of apoptotic cells in six mice was scored in randomly chosen fields under a microscope<sup>[19]</sup>.

## 2.8. Western blot

Western blotting was performed to examine the expression of apoptosis protein in tumor tissues and normal tissues. To prepare lysates of cancer tissue, about 10mg of each tumor tissue sample was incubated with 80  $\mu$ l Radio Immunoprecipitation Assay lysis buffer at 4  $^{\circ}$ C for 30 min and the lysates (30  $\mu$ g of protein per lane) were fractionated by SDS-PAGE. The proteins were electro-transferred onto poly (vinylidene fluoride) (PVDF) membranes and were detected using dilutions of the primary antibodies. The primary antibodies included caspase-3, caspase-9 (Cell Signaling, Danverse, MA) and  $\beta$ -actin (Abcam, Cambridge, MA). The PVDF membranes were washed in 0.05% Tween-20/Tris-buffered saline and then incubated with horseradish peroxidase-conjugated secondary antibody. The bound antibodies were visualized using an enhanced chemiluminescence reagent (Millipore, Billerica, MA) and quantified by densitometry using ChemiDoc XRS $\beta$  image analyzer (Bio-Rad, Hercules, CA). Densitometric analyses of bands were adjusted with  $\beta$ -actin functioning as a loading control. All experiments were performed in triplicate.

## 2.9. Statistical analysis

Statistical analysis was performed using SPSS/Win13.0

software (SPSS, Inc., Chicago, Illinois, USA). Data are presented as means $\pm$ SD and were analyzed by one-way ANOVA. Multiple between-group comparisons were performed using the S-N-K method. A *P* value <0.05 was considered statistically significant.

## 3. Results

### 3.1. Inhibitory effect of anti-VEGFR-2 ScFv-As<sub>2</sub>O<sub>3</sub>-stealth nanoparticles on hepatoma carcinoma cell growth and triggers cell apoptosis

The inhibitory effect of anti-VEGFR-2 ScFv-As<sub>2</sub>O<sub>3</sub>-stealth nanoparticles and other parallel drugs on proliferation of hepatoma carcinoma cells was examined using Bel7402 cell line. As shown in Figure 1a, the drugs had dose-dependent anti-proliferative effects on Bel7402 cells (*P*<0.05 vs. untreated control). Although the highest inhibition rate of As<sub>2</sub>O<sub>3</sub>-stealth nanoparticles was a bit higher than anti-VEGFR-2 ScFv-As<sub>2</sub>O<sub>3</sub>-stealth nanoparticles, the ID<sub>50</sub> of anti-VEGFR-2 ScFv-As<sub>2</sub>O<sub>3</sub>-stealth nanoparticles was smaller than As<sub>2</sub>O<sub>3</sub>-stealth nanoparticles. While anti-VEGFR-2 ScFv-As<sub>2</sub>O<sub>3</sub>-stealth nanoparticles and anti-VEGFR-2ScFv had almost no effects on normal liver cell line L02 (Figure 2B).

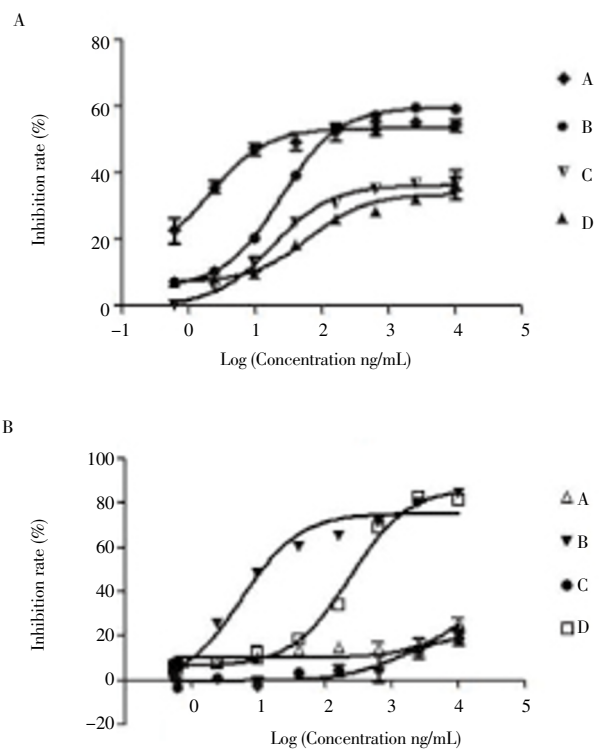


**Figure 1.** Effect of different drugs on cell proliferation.

(A) Inhibition of proliferation on Cel7402.

(B) Effects of drugs on normal liver cells L02.

A, Anti-VEGFR-2 ScFv-As<sub>2</sub>O<sub>3</sub> stealth nanoparticles group; B, As<sub>2</sub>O<sub>3</sub> stealth nanoparticles group; C, anti-VEGFR-2 ScFv; D, As<sub>2</sub>O<sub>3</sub> solution group.

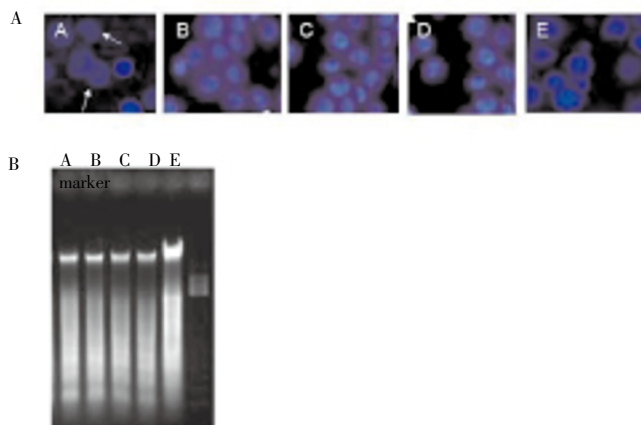


**Figure 2.** Cell apoptosis induced by different drugs. (A) Hoechst33258 staining detected the cellular morphology of Bel7402 treated by drugs; (B) DNA ladder test detected DNA fragmentation after treatment. A. Anti-VEGFR-2 ScFv-As<sub>2</sub>O<sub>3</sub> stealth nanoparticles group; B, As<sub>2</sub>O<sub>3</sub> stealth nanoparticles group; C. anti-VEGFR-2 ScFv; D, As<sub>2</sub>O<sub>3</sub> solution group; E. saline (Control).

Meanwhile, Hoechst33258 staining showed that if the nuclei showed chromatin condensation, marginalization, or appeared beaded nuclear, the cell was in the process of apoptosis. Normal cells were observed to be dispersed fluorescence, circular or oval nucleus (Figure 2A). As shown in Figure 2, the chromatin condensation and marginalization condition of cells in anti-VEGFR-2ScFv-As<sub>2</sub>O<sub>3</sub> stealth nanoparticle group was the most significant, indicating the strongest effect of triggering apoptosis of cancer cells, followed by As<sub>2</sub>O<sub>3</sub> stealth nanoparticle group, As<sub>2</sub>O<sub>3</sub> group, and anti-VEGFR-2ScFv group. The apoptosis inducing effects of different drugs was also confirmed by DNA ladder analysis (Figure 2B).

**3.2. Inhibition of hepatoma carcinoma cell invasion and migration**

The inhibitory effect of drugs on invasion and migration of hepatoma carcinoma cells was examined using an invasion assay with Matrigel-coated filters. In the absence of drug treatment (control group), Bel7402 cells displayed high invasive capability as indicated by being able to completely penetrate through the Matrigel-coated filters (Figure 3E). The activity of invasion and migration of cancer cells was markedly suppressed by a 24-h exposure.

**Table 2**

Results of blood test for PLT and WBC.

| Indexes                | A                | B                | C                | D                | E                |
|------------------------|------------------|------------------|------------------|------------------|------------------|
| PLT( $\times 10^9/L$ ) | 101.3 $\pm$ 23.4 | 102.3 $\pm$ 12.9 | 104.4 $\pm$ 19.0 | 63.3 $\pm$ 14.1* | 105.5 $\pm$ 26.5 |
| WBC( $\times 10^9/L$ ) | 7.5 $\pm$ 1.7    | 7.7 $\pm$ 1.5    | 7.8 $\pm$ 2.0    | 3.9 $\pm$ 0.9*   | 7.9 $\pm$ 1.2    |

A. Anti-VEGFR-2 ScFv-As<sub>2</sub>O<sub>3</sub> stealth nanoparticles group; B. As<sub>2</sub>O<sub>3</sub> stealth nanoparticles group; C. anti-VEGFR-2 ScFv; D. As<sub>2</sub>O<sub>3</sub> solution group; E. saline (control). Data were shown as Mean  $\pm$ SD, \**P*<0.05 vs. control.

At concentrations of 100 ng/mL of anti-VEGFR-2 ScFv-As<sub>2</sub>O<sub>3</sub>-stealth nanoparticles, As<sub>2</sub>O<sub>3</sub>-stealth nanoparticles, anti-VEGFR-2 ScFv, and As<sub>2</sub>O<sub>3</sub>, the number of cells able to penetrate through the Matrigel-coated filters was decreased by 65.4%, 50.6%, 56.5%, and 40.7%, respectively (*P*<0.01 vs. untreated control; Figure 3).

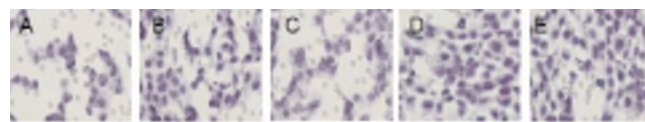


**Figure 3.** Invasive ability of cells detected using Transwell assay. A. Anti-VEGFR-2 ScFv-As<sub>2</sub>O<sub>3</sub> stealth nanoparticles group; B, As<sub>2</sub>O<sub>3</sub> stealth nanoparticles group; C. anti-VEGFR-2 ScFv; D, As<sub>2</sub>O<sub>3</sub> solution group; E. saline (Control).

**3.3. Anti-VEGFR-2 ScFv-As<sub>2</sub>O<sub>3</sub> stealth nanoparticles antitumor activity in vivo**

Tumor volumes were measured every two days since the drug administration. Our results showed that the tumor volumes in treatment group were much more smaller compared with the control group (*P*<0.01, Figure 2A). Among them, the anti-VEGFR-2 ScFv-As<sub>2</sub>O<sub>3</sub>-stealth nanoparticles treatment had the most strong inhibition effect on tumor growth (tumor weight and tumor volume were both the smallest, *P*<0.05, inhibition rate 92.9%), followed by anti-VEGFR-2 ScFv and As<sub>2</sub>O<sub>3</sub>-stealth nanoparticles, and As<sub>2</sub>O<sub>3</sub> (Figure 2B). The inhibition rates of the drugs were summarized in Table 1.

**Table 1**

Tumor weight and inhibition rate of each group.

| Indexes            | A*              | B*              | C*              | D*              |
|--------------------|-----------------|-----------------|-----------------|-----------------|
| Tumor weight(g)    | 0.30 $\pm$ 0.14 | 1.71 $\pm$ 0.07 | 1.60 $\pm$ 0.30 | 3.30 $\pm$ 0.18 |
| Inhibition rate(%) | 92.9            | 58.89           | 61.4            | 20.5            |

A. Anti-VEGFR-2 ScFv-As<sub>2</sub>O<sub>3</sub> stealth nanoparticles group; B. As<sub>2</sub>O<sub>3</sub> stealth nanoparticles group; C. anti-VEGFR-2 ScFv; D. As<sub>2</sub>O<sub>3</sub> solution group; E. saline (control). Data were shown as Mean  $\pm$ SD, \**P*<0.05 vs. control.

Blood tests showed that platelet and white blood cell count in As<sub>2</sub>O<sub>3</sub> group were significantly decreased (*P*<0.05 vs. control), while in other groups we did not notice obvious effects on blood samples, indicating that the toxicity of the other groups were not so significant (Table 2).

Meanwhile, we found through general observation that the



activity of mice in the control group was reduced, and the weight of the mice were decreased with emaciated cachexia, while the health condition of mice in treatment group were improved with basically normal activities, and condition of mice in anti-VEGFR-2 ScFv-As<sub>2</sub>O<sub>3</sub> group were significantly better compared with the other groups.

### 3.4. Inhibition of tumor growth in vivo

Tumor volumes were measured every two days since the drug administration. Our results showed that the tumor volumes in treatment group were much smaller compared with the control group ( $P < 0.01$ , Figure 4). Among them, the anti-VEGFR-2 ScFv-As<sub>2</sub>O<sub>3</sub>-stealth nanoparticles treatment had the most strong inhibition effect on tumor growth (inhibition rate 92.9%,  $P < 0.05$ ), followed by anti-VEGFR-2 ScFv and As<sub>2</sub>O<sub>3</sub>-stealth nanoparticles, and As<sub>2</sub>O<sub>3</sub> (Figure 4, Table 1).

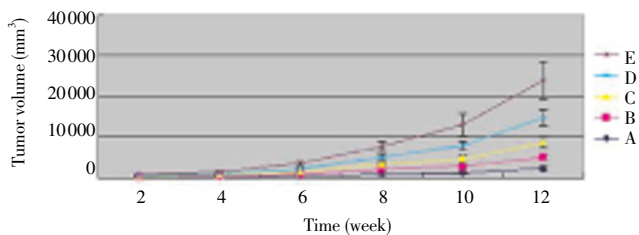


**Figure 4.** Effect of drugs on tumor volumes in different group.

A. Anti-VEGFR-2 ScFv-As<sub>2</sub>O<sub>3</sub> stealth nanoparticles group; B. As<sub>2</sub>O<sub>3</sub> stealth nanoparticles group; C. anti-VEGFR-2 ScFv; D. As<sub>2</sub>O<sub>3</sub> solution group; E. saline (Control).

Blood tests showed that platelet and white blood cell count in As<sub>2</sub>O<sub>3</sub> group were significantly decreased ( $P < 0.05$  vs. control), while in other groups we did not notice obvious effects on blood samples, indicating that the toxicity of the other groups were not so significant (Table 2).

General observation found that the activity of mice in the control group was reduced, and the weight of the mice were decreased with emaciated cachexia, while the health condition of mice in treatment group were improved with basically normal activities, and condition of mice in anti-VEGFR-2 ScFv-As<sub>2</sub>O<sub>3</sub> group were significantly better compared with the other groups.

### 3.5. Pathological and immunohistochemical results and detection of apoptosis pathway of cells in tumor tissue

Histopathologic examination further validated the inhibitory effect of anti-VEGFR-2 ScFv-As<sub>2</sub>O<sub>3</sub> on the tumorigenesis and malignant progression of liver cancer. As shown in Figure 3A a-e, anti-VEGFR-2 ScFv-As<sub>2</sub>O<sub>3</sub> stealth

nanoparticles caused the most severe necrosis of the tumor tissue, and there was barely obvious necrosis in control group. Cell apoptosis in tumor tissue was then detected by TUNEL. Data analysis showed that, the percentages of TUNEL-positive cells in anti-VEGFR-2 ScFv-As<sub>2</sub>O<sub>3</sub> stealth nanoparticles group, As<sub>2</sub>O<sub>3</sub> stealth nanoparticles group, anti-VEGFR-2 ScFvC, As<sub>2</sub>O<sub>3</sub> solution group and control group were 49.6%, 43.7%, 38.2%, 35.8%, and 19.1%, respectively ( $P < 0.05$  vs. control).

Western blotting found that the levels of caspase-3 and caspase-9 were increased in drug treatment groups, indicating that the drugs might have triggered tumor cell apoptosis through the caspase-dependent pathway (Figure 5). While in the meantime, although the caspase-3,-9 levels were also elevated in the normal liver tissues in anti-VEGFR-2ScFv-As<sub>2</sub>O<sub>3</sub>-stealth nanoparticle group, the difference was not statistically significant ( $P > 0.05$ ), and the elevated caspase-3,-9 levels might due to the small amount of free As<sub>2</sub>O<sub>3</sub> nanoparticle in the anti-VEGFR-2ScFv-As<sub>2</sub>O<sub>3</sub>-stealth nanoparticle conjugate. And in As<sub>2</sub>O<sub>3</sub> stealth nanoparticle and As<sub>2</sub>O<sub>3</sub> group the apoptotic protein caspase-3,-9 in liver tissue were both increased in a statistically significant level ( $P < 0.05$ , Figure 5C).

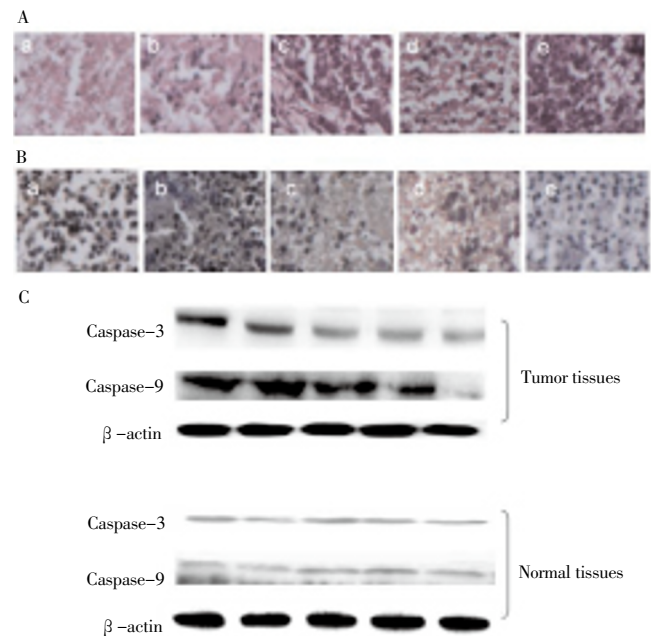


**Figure 5.** Apoptosis of tumor cells.

(A) H&E staining showed necrosis condition inside the tumor tissues. (B) TUNEL assay showed the cell apoptosis in the tissues. (C) Apoptotic protein expression detected by western blot showed that the drugs mainly affect the expression of caspase-3, -9, and almost had no effect on normal cells.

A. Anti-VEGFR-2 ScFv-As<sub>2</sub>O<sub>3</sub> stealth nanoparticles group; B. As<sub>2</sub>O<sub>3</sub> stealth nanoparticles group; C. anti-VEGFR-2 ScFv; D. As<sub>2</sub>O<sub>3</sub> solution group; E. saline (Control).

### 3.6. Microvascular density

The count of MVD in tumor tissues from anti-VEGFR-2 ScFv-As<sub>2</sub>O<sub>3</sub>, stealth nanoparticles group (5.5±1.8), As<sub>2</sub>O<sub>3</sub> stealth nanoparticles group (7.6±1.5), anti-VEGFR-2 ScFv (6.8±1.2), and As<sub>2</sub>O<sub>3</sub> solution-treated mice (8.7±0.7) was significantly decreased ( $P<0.001$ ) compared with those from control mice (12.4±2.3). MVD of anti-VEGFR-2 ScFv-As<sub>2</sub>O<sub>3</sub> stealth nanoparticles and anti-VEGFR-2 ScFv group were relatively smaller than the other two groups, indicating that the anti-VEGFR2ScFv antibody significantly improve the anti-angiogenesis effects of As<sub>2</sub>O<sub>3</sub>.

## 4. Discussion

Hepatocellular carcinoma is the most common type of liver cancer. Treatment options of HCC patients and prognosis in clinical are dependent on many factors but especially on tumor size and staging of the patients. Once diagnosed hepatocellular carcinoma usually have a poor prognosis in the late stage, only 30%–40% of patients are deemed eligible for curative intention with traditional treatment modalities including surgical resection, liver transplantation, chemoembolization and radiotherapy[20]. And there is not sufficient choice of chemotherapy drugs for the treatment of hepatocellular carcinoma, so new drug design and development for efficient drugs for HCC need to be paid more attention to in this field.

Invasion and metastasis are the most insidious and life-threatening aspects of almost all malignant cancers. Cancer invasion is initiated and maintained by several signaling pathways that control cytoskeletal dynamics and the turnover of cell-matrix and cell-cell junctions, followed by cell migration into the adjacent tissues[21]. Cancer related angiogenesis is a prerequisite for the local expansion of tumor colonies beyond the size restricted by oxygen and nutrient diffusion. Angiogenesis is related to increased metastasis formation and decreased overall survival in patients with various malignant tumors. VEGF is one of the key regulators of angiogenesis process[22]. VEGF-targeting therapies have so far shown significant benefits and been successfully integrated in routine clinical practice for several types of cancer[23]. In our study, Transwell assay showed that when VEGFR-2 was blocked by drugs, the invasion ability of cancer cells was significantly decreased, indicating that the choice of anti-VEGFR-2 as the target was a good strategy for the drug design.

As<sub>2</sub>O<sub>3</sub> is the inorganic compound with the formula As<sub>2</sub>O<sub>3</sub>, which is also an environmental toxicant as well as an effective anti-cancer agent against many types of cancers

that can produce severe side effects, such as cardiac toxicity, peripheral neuritis, gastrointestinal adverse reactions, liver, kidney failure and respiratory paralysis and even death, thus the therapeutic use of As<sub>2</sub>O<sub>3</sub> has been limited by its dose-dependent toxicity. The reasonable application of arsenic trioxide can not only avoid toxicity, but also have good effects for a number of incurable diseases. In recent years, along with clinical research, there was a good effect in some surgical syndrome, but particularly show a good development prospects in the treatment of malignant tumors[24–26].

Anti-tumor effect of As<sub>2</sub>O<sub>3</sub> has been confirmed these years with the development of *in vitro* studies, animal model, clinical trials and other aspects, and different formulations have also been studied in order to reduce its toxic side effects, which also become a hot research field in recent years. Previous studies have confirmed that As<sub>2</sub>O<sub>3</sub> could induce apoptosis of hepatoma cells and also inhibit the growth of hepatocellular carcinoma grown in nude mice[27]. However, the toxic side effects of arsenic are still worthy to be paid more attention to, which is prone to poisoning and lead to serious consequences. Antibody Drug Conjugates or ADCs are a new class of highly potent biopharmaceutical drugs designed as a Targeted therapy for the treatment of people with cancer. In design of antibody-drug conjugates, a anticancer drug such as cell toxin or cytotoxin is coupled to an antibody that specifically targets a certain tumor marker[28]. In this study we chose the nano-particles As<sub>2</sub>O<sub>3</sub> to couple with the targeting antibody anti-VEGFR-2 ScFv. For liver cancer cell line, As<sub>2</sub>O<sub>3</sub> was highly cytotoxic, and the effect of the same concentration of As<sub>2</sub>O<sub>3</sub> nanoparticles is more obvious which was also confirmed in our study. The use of anti-VEGFR-2 ScFv-As<sub>2</sub>O<sub>3</sub> stealth nanoparticles could significantly enhance the therapeutic effects while reducing the toxic side effects of As<sub>2</sub>O<sub>3</sub>.

In summary, our results showed that anti-VEGFR-2 ScFv-As<sub>2</sub>O<sub>3</sub> stealth nanoparticles could improve bioavailability, reduce drug dosage, side effects and improve efficacy when used for treatment of hepatoma cancer both *in vitro* and *in vivo*.

### Conflict of interest statement

We declare that we have no conflict of interest.

### Acknowledgements

This project was supported by Natural Science Foundation of China (81060187) and the Natural Science Foundation of

Jiangxi Province (2008GQY0050).

## References

- [1] Lin S, Hoffmann K, Schemmer P. Treatment of hepatocellular carcinoma: A systematic review. *Liver Cancer* 2012; **1**(3-4): 144-158.
- [2] Zhong JH, Li H, Li LQ, You XM, Zhang Y, Zhao YN, et al. Adjuvant therapy options following curative treatment of hepatocellular carcinoma: a systematic review of randomized trials. *Eur J Surg Oncol* 2012; **38**(4): 286-295.
- [3] El-Serag HB, Marrero JA, Rudolph L, Reddy KR. Diagnosis and treatment of hepatocellular carcinoma. *Gastroenterology* 2008; **134**(6): 1752-1763.
- [4] Franca AV, Elias Junior J, Lima BL, Martinelli AL, Carrilho FJ. Diagnosis, staging and treatment of hepatocellular carcinoma. *Braz J Med Biol Res* 2004; **37**(11): 1689-1705.
- [5] Hussain K, El-Serag HB. Epidemiology, screening, diagnosis and treatment of hepatocellular carcinoma. *Minerva Gastroenterol Dietol* 2009; **55**(2): 123-138.
- [6] Toda G, Okuaki Y. Molecular biology, diagnosis and treatment of hepatocellular carcinoma. *Nihon Naika Gakkai Zasshi* 1997; **86**(1): 146-153.
- [7] Schilsky RL. Targeted therapy for cancer: asking the right questions. *Oncology (Williston Park)* 2012; **26**(10): 947-949.
- [8] Christiansen J, Rajasekaran AK. Biological impediments to monoclonal antibody-based cancer immunotherapy. *Mol Cancer Ther* 2004; **3**(11): 1493-1501.
- [9] Alley SC, Okeley NM, Senter PD. Antibody-drug conjugates: targeted drug delivery for cancer. *Curr Opin Chem Biol* 2010; **14**(4): 529-537.
- [10] Scartozzi M, Loretelli C, Galizia E, Mandolesi A, Pistelli M, Bittoni A, et al. Role of vascular endothelial growth factor (VEGF) and VEGF-R genotyping in guiding the metastatic process in pT4a resected gastric cancer patients. *PLoS One* 2012; **7**(7): e38192.
- [11] Au WY, Kwong YL. Arsenic trioxide: safety issues and their management. *Acta Pharmacol Sin* 2008; **29**(3): 296-304.
- [12] Wang XS, Wang GY, Xu HT, Wang K, Liu M, Fu SB, et al. The effect of As<sub>2</sub>O<sub>3</sub> on induction of apoptosis and inhibition of telomerase activity in colon cancer LS-174T cells. *Zhonghua Zhong Liu Za Zhi* 2007; **29**(6): 415-418.
- [13] Zhang P. The use of arsenic trioxide (As<sub>2</sub>O<sub>3</sub>) in the treatment of acute promyelocytic leukemia. *J Biol Regul Homeost Agents* 1999; **13**(4): 195-200.
- [14] Szinicz L, Forth W. Effect of As<sub>2</sub>O<sub>3</sub> on gluconeogenesis. *Arch Toxicol* 1988; **61**(6): 444-449.
- [15] Wu MH, Lin CJ, Chen CL, Su MJ, Sun SS, Cheng AL. Direct cardiac effects of As<sub>2</sub>O<sub>3</sub> in rabbits: evidence of reversible chronic toxicity and tissue accumulation of arsenicals after parenteral administration. *Toxicol Appl Pharmacol* 2003; **189**(3): 214-220.
- [16] Xue X, Sun DF, Sun CC, Liu HP, Yue B, Zhao CR, et al. Inhibitory effect of riccardin D on growth of human non-small cell lung cancer: *in vitro* and *in vivo* studies. *Lung Cancer* 2012; **76**(3): 300-308.
- [17] Zhang XM, Lv YG, Chen GB, Zou Y, Lin CW, Yang L, et al. Effect of mild hypothermia on breast cancer cells adhesion and migration. *Biosci Trends* 2012; **6**(6): 313-324.
- [18] Zizak Z, Juranic Z, Opsenica D, Solaja BA. Mixed steroidal tetraoxanes induce apoptotic cell death in tumor cells. *Invest New Drugs* 2009; **27**(5): 432-439.
- [19] Liu HP, Gao ZH, Cui SX, Wang Y, Li BY, Lou HX, et al. Chemoprevention of intestinal adenomatous polyposis by acetyl-11-keto-beta-boswellic acid in APC(Min/+) mice. *Int J Cancer* 2013; **132**(11): 2667-2681.
- [20] Cao H, Phan H, Yang LX. Improved chemotherapy for hepatocellular carcinoma. *Anticancer Res* 2012; **32**(4): 1379-1386.
- [21] Friedl P, Alexander S. Cancer invasion and the microenvironment: plasticity and reciprocity. *Cell* 2011; **147**(5): 992-1009.
- [22] Sauter ER, Nesbit M, Watson JC, Klein-Szanto A, Litwin S, Herlyn M. Vascular endothelial growth factor is a marker of tumor invasion and metastasis in squamous cell carcinomas of the head and neck. *Clin Cancer Res* 1999; **5**(4): 775-782.
- [23] Price DJ, Miralem T, Jiang S, Steinberg R, Avraham H. Role of vascular endothelial growth factor in the stimulation of cellular invasion and signaling of breast cancer cells. *Cell Growth Differ* 2001; **12**(3): 129-135.
- [24] Antman KH. Introduction: the history of arsenic trioxide in cancer therapy. *Oncologist* 2001; **6**(Suppl 2): 1-2.
- [25] Chen GQ, Shi XG, Tang W, Xiong SM, Zhu J, Cai X, et al. Use of arsenic trioxide (As<sub>2</sub>O<sub>3</sub>) in the treatment of acute promyelocytic leukemia (APL): I. As<sub>2</sub>O<sub>3</sub> exerts dose-dependent dual effects on APL cells. *Blood* 1997; **89**(9): 3345-3353.
- [26] Thomas-Schoemann A, Batteux F, Mongaret C, Nicco C, Chereau C, Annereau M, et al. Arsenic trioxide exerts antitumor activity through regulatory T cell depletion mediated by oxidative stress in a murine model of colon cancer. *J Immunol* 2012; **189**(11): 5171-5177.
- [27] Alarifi S, Ali D, Alkahtani S, Siddiqui MA, Ali BA. Arsenic trioxide-mediated oxidative stress and genotoxicity in human hepatocellular carcinoma cells. *Onco Targets Ther* 2013; **6**: 75-84.
- [28] Qian C, Wang Y, Chen Y, Zeng L, Zhang Q, Shuai X, et al. Suppression of pancreatic tumor growth by targeted arsenic delivery with anti-CD44v6 single chain antibody conjugated nanoparticles. *Biomaterials* 2013; **34**(26): 6175-6184.